

Two-Photon Fluorescence Lysosomal Bioimaging with a Micelle-Encapsulated Fluorescent Probe

Carolina D. Andrade · Ciceron O. Yanez · Maher A. Qaddoura · Xuhua Wang ·
Curtesa L. Arnett · Sabrina A. Coombs · Jin Yu · Rania Bassiouni ·
Mykhailo V. Bondar · Kevin D. Belfield

Received: 30 September 2010 / Accepted: 28 December 2010 / Published online: 18 January 2011
© Springer Science+Business Media, LLC 2011

Abstract We report two-photon fluorescence microscopy (2PFM) imaging and in vitro cell viability of a new, efficient, lysosome-selective system based on a two-photon absorbing (2PA) fluorescent probe (**I**) encapsulated in Pluronic® F-127 micelles. Preparation of dye **I** was accomplished via microwave-assisted synthesis, resulting in improved yields and reduced reaction times. Photo-physical characterization revealed notable 2PA efficiency of this probe.

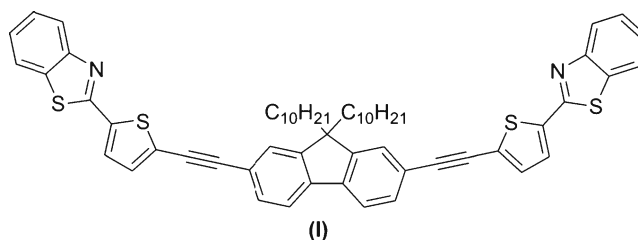
Keywords Fluorescent dyes · Pluronic · Multiphoton absorption · Bioimaging · Fluorescence microscopy · Lysosomes

C. D. Andrade · C. O. Yanez · M. A. Qaddoura · X. Wang ·
C. L. Arnett · S. A. Coombs · J. Yu · R. Bassiouni ·
K. D. Belfield (✉)
Department of Chemistry, University of Central Florida,
4000 Central Florida Boulevard,
Orlando, FL 32816, USA
e-mail: belfield@mail.ucf.edu

K. D. Belfield
CREOL, The College of Optics and Photonics,
University of Central Florida,
4000 Central Florida Boulevard,
Orlando, FL 32816, USA

M. V. Bondar
Department of Photoactivity, Institute of Physics,
National Academy of Sciences of Ukraine Prospect Nauki 46,
Kiev, Ukraine

Introduction



The advantages that 2PA materials offer over their one-photon absorbing counterparts relies on the very nature of the nonlinear absorption process, where two photons are absorbed simultaneously, offering increased 3D resolution as a result of a significantly confined excitation volume [1]. This inherent advantage has increased the interest of the scientific community in multiphoton imaging over the last decade, which has spawned the development of novel multiphoton absorbing materials and their applications. The variety of applications of these materials is witnessed in a number of fields, including microscopy [2, 3], lasing [4], and optical data storage [5–7]. In the field of bioimaging, there has been increased attention in labeling different cell components or certain cells within a specific type of tissue by direct and indirect immunostaining with efficient 2PA fluorescent dyes [8, 9].

The lysosomes and their enzymes are the centerpiece of the digestive cycle of the cell and, as such, are key in many cellular processes such as apoptosis and phagocytosis. Lysosomal activity has been associated with an array of

conditions including cancer [10], aging [11], autophagy [10, 12], and apoptotic and necrotic cell deaths [10, 13], but the specific role of the lysosomes in such processes remains a matter of some speculation. Furthermore, the less common yet still severe conditions classified as Lysosomal Storage Disorders have very serious clinical manifestations, such as mental retardation, progressive cognitive decline, and behavioral inappropriateness [14]. Thus, methods and materials to that can specifically probe lysosomes are of considerable interest.

The advent of high resolution and super resolution fluorescence microscopy techniques, including 2PFM [2], stimulated emission depletion (STED) microscopy [15, 16], photo-activated localization microscopy (PALM) [17], and interferometric photo-activated localization microscopy (iPALM) [18], have set the foundations for unforeseen resolution, and will undoubtedly lead to more exciting discoveries, especially when these techniques are combined to exploit superresolution to its very limit [19]. Even though there are commercially available alternatives for imaging the lysosomes by fluorescence, very few of the dyes or proteins employed possess the photostability and high two-photon absorption cross sections to be *efficient* 2PA probes, particularly for prolonged imaging [20].

Pluronic® F-127 has been used in drug delivery applications to enhance the solubility of hydrophobic substances such as anticancer drugs [21, 22]. Pluronic® micelles are known to be uptaken by MDCK cells by means of clathrin-mediated endocytosis when present above the critical micelle concentration (CMC) [23–25]. Probe **I** was encapsulated in Pluronic® F-127, with the purpose of it being endocytosed, and subsequently tracked through the vesicle maturation process (Fig. 1). After the micelles are endocytosed they can either reach full endosomal maturation, reaching the lysosomes, or follow exocytosis before attaining the endolysosomal stage.

Results and Discussion

The strategy for the synthesis of probe **I** is outlined in Scheme 1. Thiophene **1** underwent Sonogashira coupling with a protected terminal alkyne to yield intermediate **2** (12 h). The microwave-assisted equivalent of this reaction reached completion 360 times faster [26]. Deprotection of the triple bond in intermediate **2** was also performed under microwave irradiation, generating **3** in higher yield and shorter reaction time when compared to conventional thermal deprotection. A second Sonogashira coupling, between **3** and **4**, was required to generate probe **I**; this microwave-assisted reaction afforded the product in slightly higher yield and shorter time (20 times faster) than conventional heating (Table 1).

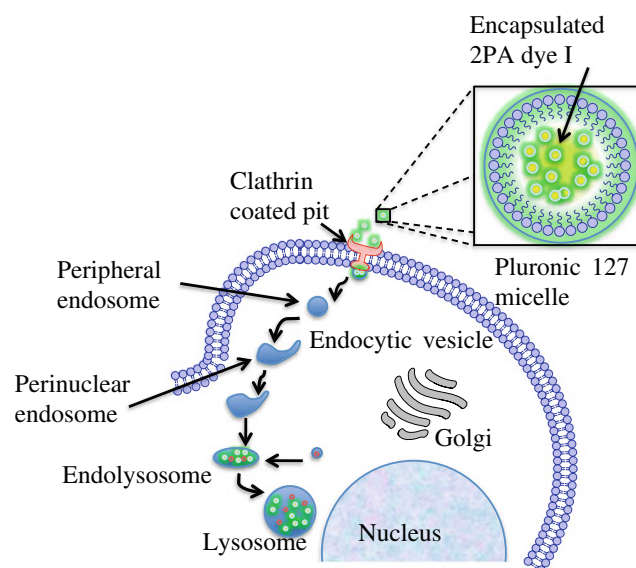
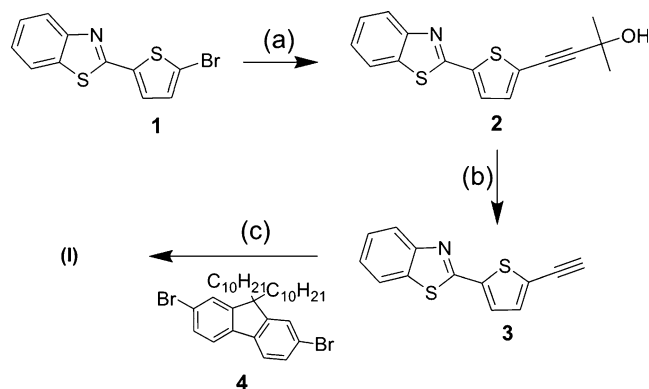


Fig. 1 Depiction of Pluronic® F-127-encapsulated 2PA probe **I** being uptaken into an HCT 116 cell by means of clathrin-mediated endocytosis. After 3 h of incubation, **I** can be found in lysosomes (see Fig. 4)

The hydrophobic character of probe **I** made it an ideal candidate for encapsulation in Pluronic® F-127. Steady state, linear absorption, and fluorescence properties of solutions of **I** in hexane and with the Pluronic® surfactant in PBS buffer were measured. Absorption maxima at around 400 nm were observed for **I** in both solvent systems. The molar extinction coefficient of **I** in hexane was determined to be around $135 \times 10^{-3} \text{ M}^{-1} \text{ cm}^{-1}$. The emission maximum shifted towards longer wavelengths when **I** was prepared in Pluronic® solution as a consequence of the increase in polarity of the media. In hexane, the fluorescence quantum yield of **I** was 0.95, while nonradiative decay led to a reduction to one third of this



Scheme 1 Microwave-assisted synthesis of 2PA probe **I**. **a**) 2-methyl-3-butyn-2-ol, Pd(PPh₃)₂Cl₂, CuI, Et₃N, toluene, thermal: reflux, 12 h (96%); microwave: 130 °C, 2 min (96%); **b**) KOH, toluene, thermal: reflux 1 h (75%); microwave: 130 °C, 8 min (98%); **c**) Pd(PPh₃)₂Cl₂, CuI, Et₃N, toluene, thermal: reflux, 20 h (55%); microwave: 130 °C, 1 h (65%)

Table 1 Variation in times and yield by using microwave irradiation for the synthesis of **I**

	Reduction in reaction time	Increase in yield
step a	360 times faster	none (96%)
step b	128 times faster	from 75% to 98%
step c	20 times faster	from 55% to 65%

value when the dye was dissolved in the aqueous Pluronic® solution (see Table 2) (Fig. 2).

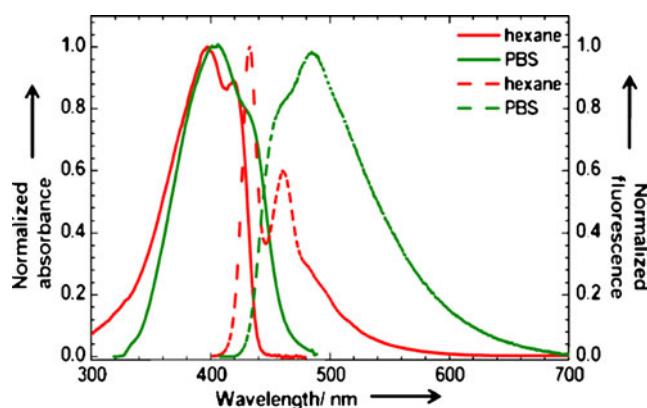
Two-photon absorption cross section values of solutions of **I** in cyclohexane, DMSO, and 5 wt% aqueous DMSO were determined using the two-photon fluorescence method from 640 to 920 nm, a convenient wavelength range for 2PFM imaging (Fig. 3). 2PA at these wavelengths was consistent for symmetrical 2PA dyes. Since adherence to the selection rules are typically more stringent for symmetrical dyes, high cross 2PA sections at twice the linear λ_{\max} are seldom observed for this type of compound (see Fig. 2) [27, 28]. The highest 2PA cross section values were observed at 680 nm for all solvents used, which is likely the maximum of the lower energy two-photon allowed transition. Even though the lowest 2PA cross sections were observed in the aqueous mixture, a value of 250 GM at ca. 700 nm is quite good. This and the fluorescence quantum yield of **I** proved favorable for 2PFM imaging.

HCT 116 cells were incubated in Pluronic® F-127 encapsulated 2PA probe **I**. A series of 0.1, 1, 10, 25, and 50 μM solutions of the micelle-encapsulated probe in culture media was prepared. Another identical series, also containing 75 nM of LysoTracker Red (Invitrogen), was prepared for colocalization studies to determine whether the micelle-encapsulated probe reached the lysosomes. HCT 116 cells were incubated in these solutions for 3 h. After fixation, the one-photon fluorescence images exhibited good agreement between the LysoTracker Red (Fig. 4b) and the Pluronic® F-127-encapsulated 2PA probe **I** (Fig. 4c), as shown by the overlay of micrographs of these two channels (Fig. 4d). The excellent colocalization agreement was further confirmed by the calculation of the colocalization coefficient which was determined to be $\cong 0.91$ [29].

Table 2 Linear optical properties of probe **I**

Compound	$\lambda_{\max}^{\text{abs}}$ (nm)	$\lambda_{\max}^{\text{em}}$ (nm)	$\Phi_{\text{F}}^{\text{[a]}}$
I in hexane ($\epsilon^{\max}=135 \times 10^{-3} \text{M}^{-1} \text{cm}^{-1}$)	397 \pm 1	433 \pm 1	0.95 \pm 0.05
I in Pluronic®F-127/PBS	403 \pm 1	485 \pm 1	0.35 \pm 0.05

^a Fluorescence quantum yield, Φ_{F} , measured relative to 9,10-diphenylanthracene in cyclohexane

**Fig. 2** Absorption (solid) and emission (broken) spectra of 2PA probe **I** in hexane (red) and encapsulated in Pluronic® F-127 (PBS solution, green)

Cell viability assays were conducted with CellTiter® 96 AQ (Promega). In this assay, the ability of the cell to metabolize MTS to formazan was evaluated [30]. Formazan has an absorption ($\lambda_{\max} \approx 490 \text{ nm}$) that is significantly red-shifted with respect to MTS. Hence, by interrogation at 490 nm, one can approximate the proportion of cells that are metabolically active or viable. To evaluate the effect of the micelle-encapsulated probe **I**, COS-7 and HCT 116 cells were seeded (5×10^3 cells/well) in a 96 well plate and incubated for 24 h in DMEM (Invitrogen). The cells were incubated with 60, 50, 25, 10, and 1 μM solutions of Pluronic® F-127-encapsulated probe **I** for 24 h. The results indicated that these concentrations did not significantly affect either cell line. Even at concentrations above those used for imaging, the cell viability is practically 100% (see Fig. 5), compelling data to support the use of this probe for in vivo two-photon fluorescence imaging.

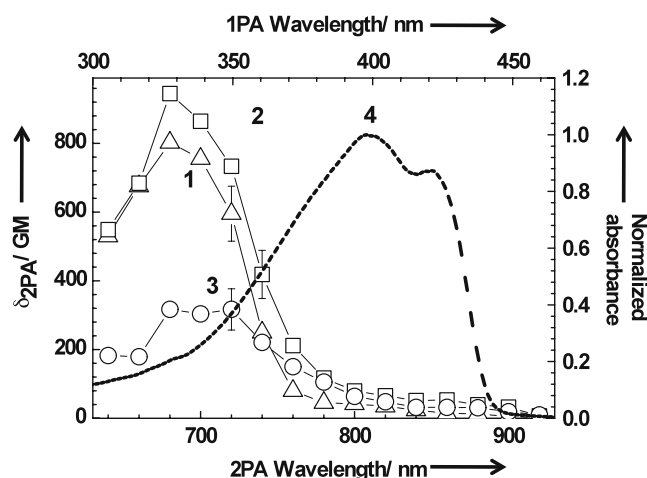
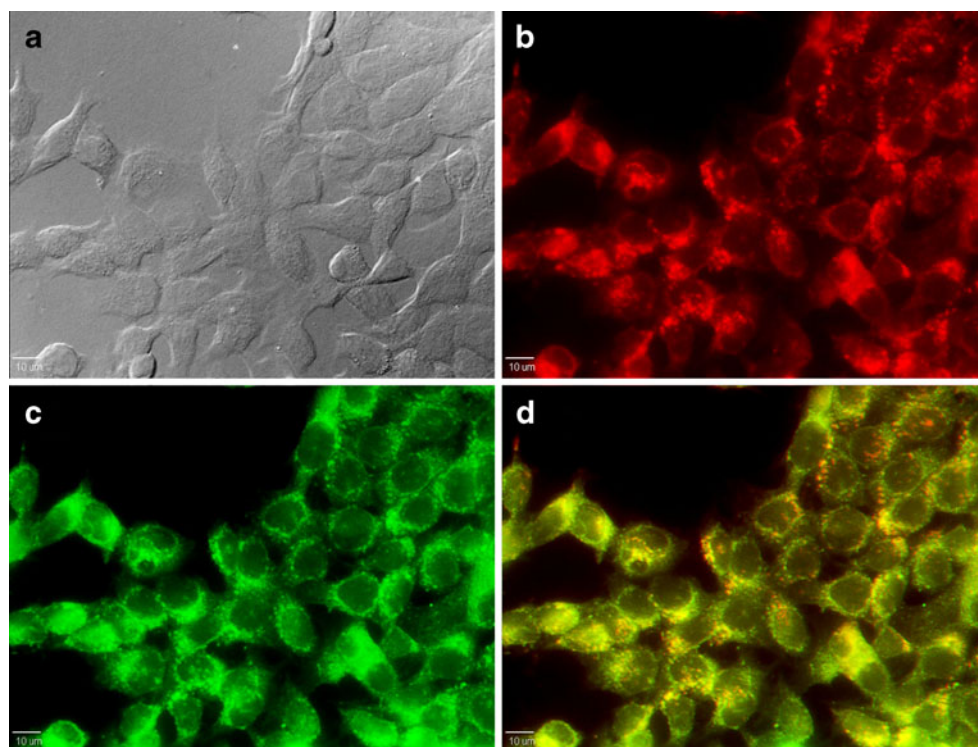
**Fig. 3** 2PA spectra of 2PA probe **I** in cyclohexane (1), DMSO (2) and 5 wt% aqueous DMSO (3). Normalized one-photon absorption spectrum of **I** in cyclohexane (4)

Fig. 4 Confocal fluorescence images of HCT 116 cells incubated with 2PA probe I encapsulated in Pluronic® F-127 (25 μ M, 3 h) and LysoTracker Red (100 nM, 3 h). DIC (a), one-photon fluorescence image showing LysoTracker Red (b) and 2PA probe I encapsulated in Pluronic® F-127 micelles (c). (d) is colocalization (overlay of B and C). 10 μ m scale bar



Two-photon fluorescence microscopy (2PFM) images of fixed HCT 116 cells incubated with probe I encapsulated in Pluronic® F-127 (50 μ M, 3 h) were collected on a modified Olympus Fluoview FV300 microscope system coupled to a tunable Coherent Mira 900 F Ti:sapphire, 76 MHz, modelocked, 200 fs laser tuned to 700 nm (Fig. 6c).

Two-photon fluorescence imaging, Fig. 6c, revealed remarkable contrast when compared to one-photon (conventional) fluorescence imaging, Fig. 6b, in which individual lysosomes become evident. This demonstrates the potential that this probe-micelle formulation has for following the endocytotic process by 2PFM. Furthermore, the versatility of this system should allow one to encapsulate a wide variety of 2PA hydrophobic dyes, an aspect of further investigation.

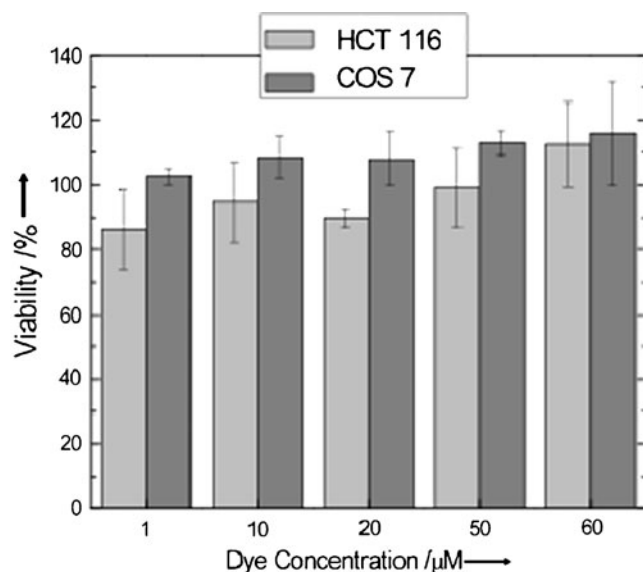


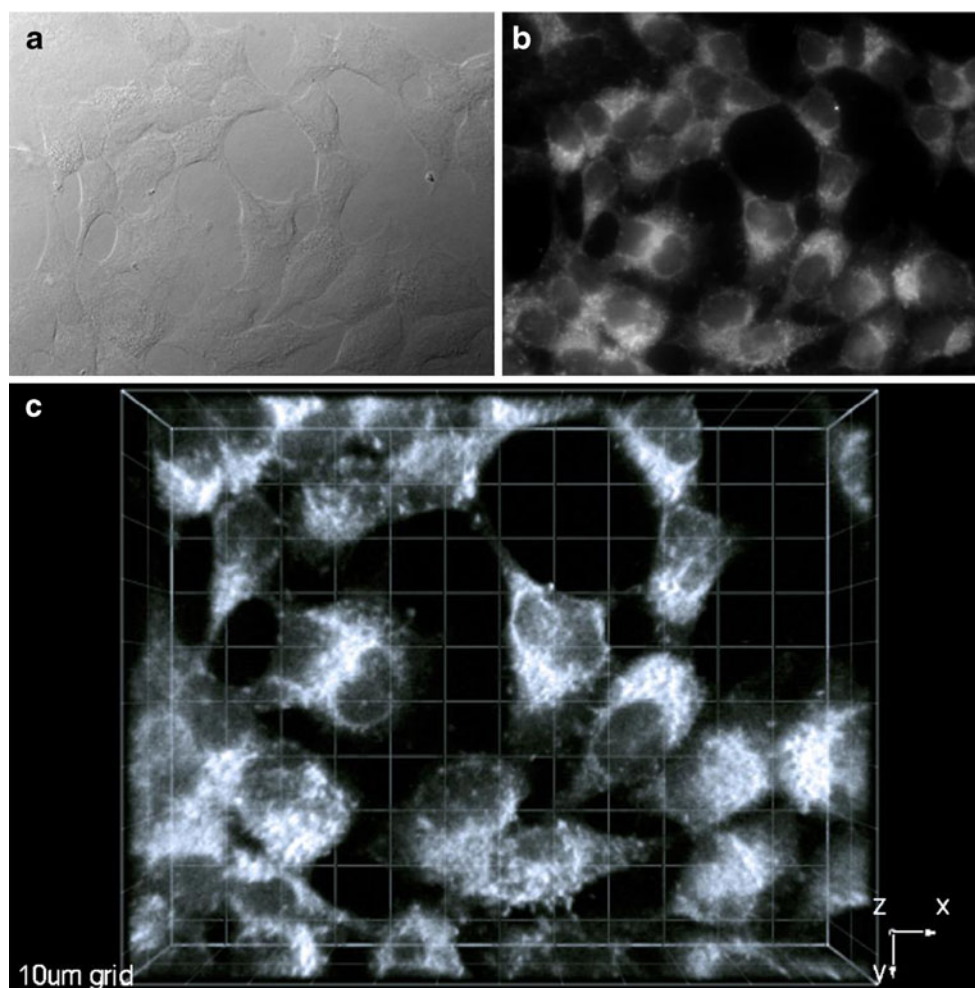
Fig. 5 Cell viability assays of COS-7 and HCT 116 cells incubated with Pluronic® F-127-encapsulated 2PA probe I

Experimental Section

Materials and Methods

2-(5-Bromothiophen-2-yl)benzothiazole **1** and 2,7-dibromo-9,9-didecyl-9 H-fluorene **4** were prepared as described previously [31, 32]. Synthesis of compounds **3** and **4** has been achieved previously by conventional heating, and dye **I** was prepared through a different methodology [33]. All microwave reactions were carried out under N_2 in a CEM Discover unit microwave in 10 mL closed vessels programmed at a maximum temperature of 130 $^{\circ}C$, maximum pressure of 100 psi and maximum power of 100 Watts. All other reagents and solvents were used as received from commercial suppliers. 1H and ^{13}C NMR spectra were recorded in $CDCl_3$ on a Varian NMR spectrometer at 500 and 125 MHz, respectively. Elemental analyses were performed by Atlantic Microlab, Inc.

Fig. 6 One- and two-photon fluorescence micrographs of HCT 116 cells incubated with probe I encapsulated in Pluronic® F-127 (50 μ M, 3 h). DIC (a), one-photon fluorescence (b), and 3D reconstruction from overlaid 2PFM images (c), 76 MHz, 200 fs laser 700 nm, 60x objective (NA=1.35, Olympus). Scale: 10 μ m grid



Synthetic Procedures and Characterization

Synthesis of 4-(5-(benzothiazol-2-yl)thiophen-2-yl)-2-methylbut-3-yn-2-ol (2) 2-(5-Bromothiophen-2-yl)benzothiazole **1** (200 mg, 0.67 mmol), 2-methyl-3-butyn-2-ol (170 mg, 2.02 mmol), Pd(PPh₃)₂Cl₂ (19 mg, 0.027 mmol) and CuI (5 mg, 0.027 mmol) were dissolved in a 1:4 mixture of Et₃N:toluene (5 mL). The mixture was either heated under reflux for 12 h or irradiated in the microwave for 2 min, when it was determined by TLC that the reaction was completed. The mixture was filtered through a celite plug, and purified by column chromatography using as a solvent a mixture of hexane:ethyl acetate (1:1) to yield 192 mg (96%) of a pale yellow solid when the heating was achieved by either method. m.p. 163.9–164.6 °C. ¹H NMR (500 MHz, CDCl₃) δ 8.02 (d, *J*=8.04 Hz, 1 H, Ph-H), 7.85 (d, *J*=7.87 Hz, 1 H, Ph-H), 7.50 (d, *J*=3.95 Hz, 1 H, Thy-H), 7.47 (m, 1 H, Ph-H), 7.38 (m, 1 H, Ph-H), 7.18 (d, *J*=3.95 Hz, 1 H, Thy-H), 2.11 (s, 1 H, -OH), 1.64 (s, 6 H, CH₃). ¹³C NMR (125 MHz, CDCl₃) δ 160.4, 153.6, 137.8, 134.7, 132.9, 128.3, 126.4, 125.3, 123.1,

121.5, 121.4, 100.2, 75.2, 65.8, 31.3. Anal. Calcd for C₁₆H₁₃NOS₂: C, 64.18; H, 4.38; N, 4.68. Found: C, 64.10; H, 4.33; N, 4.64.

Synthesis of 2-(5-ethynylthiophen-2-yl)benzothiazole (3) 4-(5-(Benzothiazol-2-yl)thiophen-2-yl)-2-methylbut-3-yn-2-ol **2** (300 mg, 1.0 mmol) and KOH (300 mg, 5.3 mmol) were heated either under reflux for 1 h or under microwave irradiation for 8 min. The mixture was filtered, and then purified by column chromatography using as a solvent hexane to yield 180 mg (75%) by the conventional heating method or 236 mg (98%) by the microwave assisted method of a pale yellow solid. m.p. 117.3–118.3 °C. ¹H NMR (500 MHz, CDCl₃) δ 8.03 (d, *J*=8.21 Hz, 1 H, Ph-H), 7.86 (d, *J*=8.21 Hz, 1 H, Ph-H), 7.51 (d, *J*=3.94 Hz, 1 H, Thy-H), 7.48 (m, 1 H, Ph-H), 7.39 (m, 1 H, Ph-H), 7.28 (d, *J*=3.94 Hz, 1 H, Thy-H), 3.50 (s, 1 H, C≡C-H). ¹³C NMR (125 MHz, CDCl₃) δ 160.2, 153.6, 138.5, 134.8, 133.9, 133.7, 127.8, 126.5, 125.4, 123.2, 121.6, 84.0, 76.5. Anal. Calcd for C₁₃H₇NS₂: C, 64.70; H, 2.92; N, 5.80. Found: C, 64.64; H, 2.91; N, 5.75.

Synthesis of 2,2'-(5,5'-(9,9-didecyl-9 H-fluorene-2,7-diyl)bis(ethyne-2,1-diyl)bis(thiophene-5,2-diyl))dibenzothiazole (I) 2,7-Dibromo-9,9-didecyl-9 H-fluorene **4** (300 mg, 0.50 mmol), 2-(5-ethynylthiophen-2-yl)benzothiazole **3** (263 mg, 1.09 mmol), Pd(PPh₃)₂Cl₂ (30 mg, 0.04 mmol) and CuI (8 mg, 0.04 mmol), were dissolved in a 1:4 mixture of Et₃N:toluene (5 mL). The mixture was heated under reflux for 12 h or in the microwave for 1 h. The mixture was filtered through a celite plug, and purified by column chromatography using as a solvent a mixture of hexane:ethyl acetate (10:1) to yield 252 mg (55%) of a yellow solid by conventional heating and 298 mg (65%) when microwave irradiation was used. m.p. 74.0–75.5 °C. ¹H NMR (500 MHz, CDCl₃) δ 8.04 (dd, *J*=8.09 Hz, *J*=0.54 Hz, 2 H, Ph-H), 7.87 (dd, *J*=8.04 Hz, *J*=0.53 Hz, 2 H, Ph-H), 7.70 (d, *J*=7.83 Hz, 2 H, Ph-H), 7.57 (d, *J*=3.89 Hz, 1 H, Thy-H), 7.55 (m, 2 H, Ph-H), 7.53 (m, 2 H, Ph-H), 7.49 (m, 2 H, Ph-H), 7.39 (m, 2 H, Ph-H), 7.31 (d, *J*=3.89 Hz, 1 H, Thy-H), 2.00 (m, 4 H, CH₂), 1.15 (m, 28 H, CH₂), 0.84 (t, *J*=6.96 Hz, 6 H, CH₃), 0.61 (m, 4 H, CH₂). ¹³C NMR (125 MHz, CDCl₃) δ 160.5, 153.7, 151.3, 141.1, 138.0, 134.7, 132.6, 130.8, 128.4, 127.1, 126.6, 125.9, 125.5, 123.1, 121.5, 121.3, 120.2, 97.0, 82.8, 55.4, 40.3, 31.9, 30.0, 29.6, 29.5, 29.3, 29.3, 23.8, 22.7, 14.1. Anal. Calcd for C₅₉H₆₀N₂S₄: C, 76.58; H, 6.54; N, 3.03. Found: C, 76.79; H, 6.75; N, 2.79.

Encapsulation of I in Pluronic® F-127 A solution containing 25 mg of Pluronic® F-127 in 10 mL of PBS buffer (pH=7.4) was mixed with a solution containing dye **I** (5 mg) in CH₂Cl₂ (10 mL). The organic solvent was allowed to evaporate at room temperature overnight. The mixture was filtered through a Whatman 2 μm pore size disposable filter to generate a fluorescent yellow solution.

Measurements

Absorption spectra were recorded with an Agilent 8453 UV–visible spectrophotometer. Steady-state fluorescence spectra were measured at room temperature with a PTI Quantamaster spectrofluorimeter in the photon counting regime of the PMT using an L-format configuration. The fluorescence spectra were corrected for the spectral dependence of the PMT. All measurements were performed in hexane at room temperature in 1 cm quartz cuvettes, with dye concentrations in the order of 10⁻⁶ M. Fluorescence quantum yields were determined relative to 9, 10-diphenylanthracene in cyclohexane as a standard.

Two-photon absorption spectra of **I** were measured at 700, 750 and 800 nm in spectroscopic grade nonpolar cyclohexane, polar DMSO and aqueous mixtures by a typical two-photon fluorescence 2PF method relative to

Rhodamine B in methanol as a standard [34]. The setup comprised a PTI QuantaMaster spectrofluorimeter coupled to a femtosecond Clark-MXR CPA-2010 laser that pumped optical parametric generator/amplifiers (TOPAS) with tuning range 600–950 nm, pulse duration ≈ 140 fs (FWHM), 1 kHz repetition rate and pulse energies up to ~ 0.15 μJ. Two-photon fluorescence measurements were performed in 10 mm quartz cuvettes with dye concentrations ~10⁻⁵ M. The values of 2PA cross section, δ_{2PA}, were determined by the equation [35]:

$$\delta_{2PA}^S = \delta_{2PA}^R \cdot \frac{\langle F(t) \rangle_S \cdot C_R \cdot \Phi_R \cdot \varphi_R \cdot \langle P(t) \rangle_R^2}{\langle F(t) \rangle_R \cdot C_S \cdot \Phi_S \cdot \varphi_S \cdot \langle P(t) \rangle_S^2} \quad (1)$$

where $\langle F(t) \rangle$, $\langle P(t) \rangle$, *C* and Φ , are the averaged fluorescence intensity, excitation power, molecular concentration and geometric factor, respectively. Subscripts *S* and *R* refer to the sample and reference compound. The quadratic dependence of 2PF intensity on the excitation power was checked for every excitation wavelength, λ_{ex}, and special attention was paid to verify the independence of the fluorescence quantum yield from λ_{ex}.

Cell Culture and Incubation

HCT 116 cell were cultured in DMEM, supplemented with 10% FBS, and 1% penicillin, 1% streptomycin, at 37 °C, under 5% CO₂ environment. N° 1 round 12 mm coverslips were treated with poly-D-lysine, to improve cell adhesion, and washed (3×) with PBS buffer solution. The treated cover slips were placed in 24-well plates and 80,000 cells/well were seeded and incubated at the same conditions as indicated above until 75%–85% confluency was reached on the coverslips. From a 3.03 × 10⁻⁴ M stock solution of Pluronic® F-127 encapsulated dye **I** a series of 0.1, 1, 10, 25, and 50 μM solutions in culture media were made all of them also containing 75 nM of LysoTracker Red (Invitrogen). These solutions were used to incubate the cells for 3 h. The dye solutions were extracted and the coverslipped cells were washed abundantly with PBS (4×).

Cell fixing and mounting: Cells were fixed with 3.7% solution of paraformaldehyde in pH 7.4 PBS buffer for 10 min. The fixing agent was extracted and washed (2×) with PBS. To reduce autofluorescence, a fresh solution of NaBH₄ (1 mg/mL) in pH=8 PBS buffer was used to treat the fixed cells (2×). The coverslipped cells were then washed with buffer PBS (2×) and mounted on microscope slides using Prolong Gold (Invitrogen) as a mounting media.

Cell Viability

Cell viability was assessed with CellTiter® 96 AQ (Promega). COS-7 and HCT 116 cells were seeded (5 ×

10^3 cells/well) in a 96 well plate and incubated for 24 h in 90 μ L of DMEM (Invitrogen) without phenol red, supplemented with 10% FBS (Atlanta Biologicals), and 1% penicillin-streptomycin. The cell was incubated for an additional 24 h with 60, 50, 25, 10 and 1 μ M solutions of Pluronic® F-127-encapsulated dye **I** in FBS complemented (10%) culture media. Then 20 μ M of the CellTiter® 96 AQ reagent was added into each well and subsequently incubated for another 4 h, 37 °C after which the respective absorbance values were read on a SpectraMax M5 plate reader (Molecular Devices) at 490 nm to determine the relative amount of formazan produced [30]. Cell viability% was calculated by the following expression:

$$\text{Cell viability (\%)} = \frac{\text{Abs}_{490\text{nm}}^{\text{S}} - \text{Abs}_{490\text{nm}}^{\text{B}}}{\text{Abs}_{490\text{nm}}^{\text{C}} - \text{Abs}_{490\text{nm}}^{\text{B}2}} \times 100\% \quad (2)$$

where $\text{Abs}_{490\text{nm}}^{\text{S}}$ is the absorbance of the cells at the different concentrations of micelle encapsulated dye **I**, $\text{Abs}_{490\text{nm}}^{\text{B}}$ is the absorbance of a cell-free well containing only encapsulated dye **I** in at the concentrations that were studied, $\text{Abs}_{490\text{nm}}^{\text{C}}$ is the absorbance of cells incubated in media without any other component, and $\text{Abs}_{490\text{nm}}^{\text{B}2}$ is the absorbance of a cell-free well.

Confocal One-Photon Fluorescence Imaging

One-photon fluorescence microscopy images were recorded on an Olympus IX-81 confocal microscope equipped with a Hamamatsu EM-CCD C9100 digital camera. One-photon confocal fluorescence images of the fixed cells were taken using a custom made filter cube (Ex:377/50; DM: 409; Em:525/40) and a Texas Red filter cube (Ex:562/40; DM: 593; Em:624/40) for dye **I** and LysoTracker Red, respectively.

Two-Photon Upconverted Fluorescence Imaging

Two-photon fluorescence imaging was performed on a modified Olympus Fluoview FV300 laser scanning confocal microscopy system equipped with a broadband, tunable Coherent Mira Ti:sapphire laser (115 fs pulse width, 76 MHz repetition rate), pumped by a 10 W Coherent Verdi frequency doubled Nd:YAG laser. The laser was tuned and modelocked to 700 nm and used as the two-photon excitation source. The two-photon induced fluorescence was collected by a 60 \times microscope objective (UPLANSAPO 60 \times , N.A.=1.35 Olympus). A high transmittance (>95%) short-pass filter (cutoff 685 nm, Semrock) was placed in front of the PMT detector within the FV300 scanhead in order to filter off background radiation from the laser source (700 nm).

Conclusions

Encapsulation of hydrophobic 2PA probe **I** in Pluronic® F-127 is a viable method for delivering the fluorescent probes into the lysosomes of HCT 116 cells. After photo-physical characterization, the fluorene-based fluorescent probe **I** proved to have high 2PA cross sections in polar solvents, and good fluorescence quantum yields. The yields and reaction times of this probe were significantly improved by the use of microwave-assisted synthetic procedures. 2PFM imaging revealed remarkable contrast when compared to the one-photon fluorescence, suggesting the potential that this probe-micelle formulation has in bioimaging. Cell viability assays, carried out for HCT 116 and COS-7 cells, indicate that the probe concentrations used for imaging purposes are virtually harmless to HCT 116 and COS-7 cells.

Acknowledgments This work was supported by the National Institutes of Health (1 R15 EB008858-01), the National Science Foundation (CHE-0832622 and CHE-0840431), the US Civilian Research and Development Foundation (UKB2-2923-KV-07), and the Ministry of Education and Science of Ukraine (grant M/49-2008).

References

- Göppert-Mayer M (1931) Über Elementarakte mit zwei Quantensprüngen. *Ann Phys* 401:273–294
- Denk W, Strickler JH, Webb WW (1990) 2-photon laser scanning fluorescence microscopy. *Science* 248:73–76
- Schafer-Hales KJ, Belfield KD, Yao S, Frederiksen PK, Hales JM, Kolattukudy PE (2005) Fluorene-based fluorescent probes with high two-photon action cross-sections for biological multiphoton imaging applications. *J Biom Opt* 10:051402-1–051402-8
- Belfield KD, Bondar MV, Yanez CO, Hernandez FE, Przhonska OV (2009) Two-photon absorption and lasing properties of new fluorene derivatives. *J Mater Chem* 19:7498–7502
- Corredor CC, Huang ZL, Belfield KD (2006) Two-photon 3D optical data storage via fluorescence modulation of an efficient fluorene dye by a photochromic diarylethene. *Adv Mater* 18:2910–2914
- Corredor CC, Huang ZL, Belfield KD, Morales AR, Bondar MV (2007) Photochromic polymer composites for two-photon 3D optical data storage. *Chem Mater* 19:5165–5173
- Yanez CO, Andrade CD, Yao S, Luchita G, Bondar MV, Belfield KD (2009) Photosensitive polymeric materials for two-photon 3D WORM optical data storage systems. *ACS Appl Mater Interfaces* 1:2219–2229
- Morales AR, Schafer-Hales KJ, Marcus AI, Belfield KD (2008) Amine-reactive fluorene probes: synthesis, optical characterization, bioconjugation, and two-photon fluorescence imaging. *Bioconjug Chem* 19:2559–2567
- Morales AR, Yanez CO, Schafer-Hales KJ, Marcus AI, Belfield KD (2009) Biomolecule labeling and imaging with a new fluorenyl two-photon fluorescent probe. *Bioconjug Chem* 20:1992–2000
- Levine B (2007) Cell biology—Autophagy and cancer. *Nature* 446:745–747
- Bahr BA, Bendiske J (2002) The neuropathogenic contributions of lysosomal dysfunction. *J Neurochem* 83:481–489

12. Levine B, Wei YJ, Becker N, Anderson M (2009) Molecular regulation of the autophagy function of Beclin 1. *Autophagy* 5:906
13. Sinha S, Levine B (2008) The autophagy effector Beclin 1: a novel BH3-only protein. *Oncogene* 27:S137–S148
14. Walkley SU (1998) Cellular pathology of lysosomal storage disorders. *Brain Pathol* 8:175–193
15. Donnert G, Keller J, Medda R, Andrei MA, Rizzoli SO, Lurmann R, Jahn R, Eggeling C, Hell SW (2006) Macromolecular-scale resolution in biological fluorescence microscopy. *Proc Natl Acad Sci USA* 103:11440–11445
16. Hell SW, Wichmann J (1994) Breaking the diffraction resolution limit by stimulated-emission—stimulated-emission-depletion fluorescence microscopy. *Opt Lett* 19:780–782
17. Betzig E, Patterson GH, Sougrat R, Lindwasser OW, Olenych S, Bonifacino JS, Davidson MW, Lippincott-Schwartz J, Hess HF (2006) Imaging intracellular fluorescent proteins at nanometer resolution. *Science* 313:1642–1645
18. Shtengel G, Galbraith JA, Galbraith CG, Lippincott-Schwartz J, Gillette JM, Manley S, Sougrat R, Waterman CM, Kanchanawong P, Davidson MW, Fetter RD, Hess HF (2009) Interferometric fluorescent super-resolution microscopy resolves 3D cellular ultrastructure. *Proc Natl Acad Sci USA* 106:3125–3130
19. Belfield KD, Bondar MV, Yanez CO, Hernandez FE, Przhonska OV (2009) One- and two-photon stimulated emission depletion of a sulfonyl-containing fluorene derivative. *J Phys Chem B* 113:7101–7106
20. Wang X, Nguyen DM, Yanez CO, Rodriguez L, Ahn H-Y, Bondar MV, Belfield KD (2010) High fidelity hydrophilic probe for two-photon fluorescence lysosomal imaging. *J Am Chem Soc* 132:12237–12239
21. Batrakova EV, Kabanov AV (2008) Pluronic block copolymers: evolution of drug delivery concept from inert nanocarriers to biological response modifiers. *J Control Release* 130:98–106
22. Escobar-Chavez JJ, Lopez-Cervantes M, Naik A, Kalia YN, Quintanar-Guerrero D, Ganem-Quintanar A (2006) Applications of thermoreversible pluronic F-127 gels in pharmaceutical formulations. *J Pharm Pharmaceut Sci* 9:339–358
23. Sahay G, Batrakova EV, Kabanov AV (2008) Different internalization pathways of polymeric micelles and unimers and their effects on vesicular transport. *Bioconjug Chem* 19:2023–2029
24. Kabanov AV, Levashov AV, Alakhov VY (1989) Lipid modification of proteins and their membrane-transport. *Protein Eng* 3:39–42
25. Batrakova EV, Li S, Vinogradov SV, Alakhov VY, Miller DW, Kabanov AV (2001) Mechanism of pluronic effect on P-glycoprotein efflux system in blood-brain barrier: contributions of energy depletion and membrane fluidization. *J Pharmacol Exp Ther* 299:483–493
26. Yanez CO, Andrade CD, Belfield KD (2009) Characterization of novel sulfonium photoacid generators and their microwave-assisted synthesis. *Chem Commun* 827–829
27. Belfield KD, Bondar MV, Przhonska OV, Schafer KJ (2002) Steady-state spectroscopic and fluorescence lifetime measurements of new two-photon absorbing fluorene derivatives. *J Fluoresc* 12:449–454
28. Belfield KD, Bondar MV, Hales JM, Morales AR, Przhonska OV, Schafer KJ (2005) One- and two-photon fluorescence anisotropy of selected fluorene derivatives. *J Fluoresc* 15:3–11
29. Manders EMM, Verbeek FJ, Aten JA (1993) Measurement of colocalization of objects in dual-color confocal images. *J Microsc* 169:375–382
30. Cory AH, Owen TC, Barltrop JA, Cory JG (1991) Use of an aqueous soluble tetrazolium formazan assay for cell-growth assays in culture. *Cancer Comment* 3:207–212
31. Zeng DX, Chen Y (2007) A selective, fluorescent probe for Hg²⁺ detection in aqueous solution. *J Photochem Photobiol A* 186:121–124
32. Belfield KD, Yao S, Morales AR, Hales JM, Hagan DJ, Van Stryland EW, Chapela VM, Percino J (2005) Synthesis and characterization absorbing polymers of novel rigid two-photon. *Polym Adv Technol* 16:150–155
33. Andrade CD, Yanez CO, Rodriguez L, Belfield KD (2010) A series of fluorene-based two-photon absorbing molecules: synthesis, linear and nonlinear characterization, and bioimaging. *J Org Chem* 75:3975–3982
34. Makarov NS, Drobizhev M, Rebane A (2008) Two-photon absorption standards in the 550–1600 nm excitation wavelength range. *Opt Express* 16:4029–4047
35. Albota MA, Xu C, Webb WW (1998) Two-photon fluorescence excitation cross sections of biomolecular probes from 690 to 960 nm. *Appl Opt* 37:7352–7356